Reduced Auditory Steady State Responses in Autism Spectrum Disorder

Seymour, R.A[1,2]., Rippon, G[1]., Gooding-Williams, G[1],. Sowman, P.F.[2] & Kessler, K[1].

[1] Aston Neuroscience Institute, School of Life and Health Sciences, Aston University, Birmingham, B4 7ET.

[2] Department of Cognitive Science, Macquarie University, Sydney, Australia, 2109.

robert.seymour@mq.edu.au @robbyseymour

k.kessler@aston.ac.uk

Keywords: **Auditory Steady State; Autism Spectrum Disorder; MEG; Gamma; Sensory;**

Abstract

Background: Auditory steady state responses (ASSRs) are elicited by clicktrains or amplitude-modulated tones, which entrain auditory cortex at their specific modulation rate. Previous research has reported reductions in ASSRs at 40Hz for autism spectrum disorder (ASD) participants and first-degree relatives of people diagnosed with ASD [1,2].

Methods: Using a 1.5s-long auditory clicktrain stimulus, designed to elicit an ASSR at 40Hz, this study attempted to replicate and extend these findings. Magnetencephalography (MEG) data were collected from 18 adolescent ASD participants and 18 typically developing controls.

Results: The ASSR localised to bilateral primary auditory regions. Regions of interest were thus defined in left and right primary auditory cortex (A1). While the transient gamma-band response (tGBR) from 0-0.3s following presentation of the clicktrain stimulus was not different between groups, for either left or right A1, the ASD group had reduced oscillatory power at 40Hz from 0.3 to 1.5s post-stimulus onset, for both left and right A1. Additionally, the ASD group had reduced inter-trial coherence (phase consistency over trials) at 40Hz from 0.5-1.0s for right A1 and 0.9-1.1s for left A1.

Limitations: In this study, we did not conduct a clinical autism assessment (e.g. the ADOS), and therefore it remains unclear whether ASSR power and/or ITC are associated with the clinical symptoms of ASD.

Conclusion: Overall, our results support a specific reduction in ASSR oscillatory power and inter-trial coherence in ASD, rather than a generalised deficit in gamma-band responses. We argue that this could reflect a developmentally relevant reduction in non-linear neural processing.

Background

Autism Spectrum Disorder (ASD) is a neurodevelopmental condition characterised by impairments in social interaction, disrupted communication and repetitive behaviours [3]. Although these features remain the primary diagnostic markers of ASD, the presence of sensory symptoms has recently been given a more central diagnostic role. This change in symptom emphasis reflects the observation that over 90% of ASD individuals experience hyper- and/or hypo-sensitive sensory perception [4,5]. It has been suggested that differences in low-level sensory processing contribute to the atypical developmental trajectories of higher-level cognitive functions in autism [6]. An understanding of the neural circuits involved will therefore prove fruitful for ASD research, and could even facilitate the developmental of earlier diagnostic markers [7,8].

Dysregulated neural oscillations are a promising neural correlate of atypical sensory processing in ASD. In particular, differences in high frequency gamma-band oscillations (30-80Hz) have been reported in ASD across visual, auditory and somatosensory domains [7,9–13]. Gamma oscillations are generated through excitatory-inhibitory (E-I) neuronal coupling [14], which facilitates periods of pre and post-synaptic excitability alignment, thereby promoting efficient neural communication [15]. Findings of atypical gamma oscillations in ASD may therefore reflect disrupted E-I interactions within cortical micro-circuits [16], and concomitant effects on local and global brain connectivity [17].

Within the context of auditory processing, findings of dysregulated gamma-band oscillations in ASD have been previously reported [7]. One prevalent approach to study auditory gamma-band activity non-invasively, is through amplitude modulated tones called “clicktrains”. Such stimuli produce two distinct gamma-band responses. First, a transient gamma-band response (tGBR) is generated within the first 0.3 seconds after stimulus onset [18]. This tGBR is broadband (30-60Hz) and generated in primary and secondary auditory cortices. Second, clicktrain stimuli produce an auditory steady-state response (ASSR), in which neural populations in primary auditory regions are entrained to the modulation frequency for the duration of the clicktrain [19]. In adults, the entrainment in primary auditory cortex is greatest for clicktrains modulated at 40Hz [20]. Measures of inter-trial coherence (ITC) can also be used to measure the ASSR, by quantifying the degree of phase consistency across trials [21]. One advantage of ASSRs is their high test re-test reliability which approaches an intraclass correlation of 0.96, even with a relatively small number of trials [22,23]. Furthermore, ASSRs are modulated by neural development, increasing in power by approximately 0.01 ITC value per year, until early adulthood [24,25], potentially linked with the maturation of superficial cortical layers [26,27]. This makes the ASSR an ideal tool for studying auditory function in developmental conditions like ASD.

Two studies to date have measured ASSRs in an ASD context, that is, in ASD participants and in the first-degree relatives of people diagnosed with ASD. Wilson & colleagues (2007) reported a reduction in left-hemisphere auditory ASSR power in a group of 10 autistic adolescents, using an early 37-channel MEG system [2]. The second study reported reduced ITC in first-degree relatives of people diagnosed with ASD, with maximal reductions at 40Hz across both hemispheres [1]. Reductions in the ASSR could therefore be an ASD-relevant endophenotype. Additionally, the finding of reduced ITC suggests that dysregulated phase dynamics in bilateral primary auditory cortex could underlie reductions in the ASSR in ASD. However, measures of ITC have not been applied to study the ASSR directly in a

group of autistic participants. Additionally, it remains unclear whether reductions in ASSRs are bilateral [1] or unilateral [2] in nature.

This study attempted to replicate and extend previous findings showing differences in ASSR responses in autism [1,2]. Data were collected from a group of 18 adolescent ASD participants and 18 typically developing controls using a 306-channel MEG system (Elekta Neuromag). An auditory clicktrain stimulus was presented binaurally to participants, to elicit bilateral ASSRs at 40Hz. To investigate prolonged neural entrainment, clicktrain stimuli were presented for a total of 1.5, rather than 0.5s like previous studies [1,2]. ASSRs were analysed over frequency *and* time, in order to investigate transient changes in 40Hz power and inter-trial coherence. It was hypothesised that compared with the control group, the ASD group would show reduced ASSR power and ITC at 40Hz for the duration of clicktrain presentation [1,2]. As discussed above, clicktrain stimuli also elicit a broadband, transient gamma-band response (tGBR) within the first 0.3s post-stimulus onset [18]. Given findings of reduced tGBRs in ASD [8] in response to sinusoidal tones, this study examined the tGBR alongside the sustained ASSR at 40Hz.

Methods

Participants

Data were collected from 18 participants diagnosed with ASD and 18 age-matched typically developing controls, see Table 1. ASD participants had a confirmed clinical diagnosis of ASD or Asperger's syndrome from a paediatric psychiatrist. Participants were excluded if they were taking psychiatric medication or reported epileptic symptoms. Control participants were excluded if a sibling or parent was diagnosed with ASD. Data from a further 9 participants were excluded, see *Supporting Information.*

	N	Age	Male/Female	Autism Quotient (Adult) /50	Raven Matrices Score /60	Glasgow Sensory Score /168	Mind in the Eyes Score /36
ASD	18	Mean = 16.67; SD = 3.2; Range = 14-20	14 M; 4 F	Mean = 32.60*; SD = 6.64; Range = 21-46	Mean = 43.84; SD = 7.93; Range = 27-56	Mean = 65.33*; SD = 27.69; Range = 27-126	Mean = 21.88; SD = 4.87; Range = 12-30
Control	18	Mean = 16.89; SD = 2.8; Range = 14-20	15 M; 3 F	Mean = 10.91; SD = 5.43; Range = 6-21	Mean = 48.71; SD = 5.78; Range = 37-56	Mean = 38.70; SD = 6.88; Range = 29-50	Mean = 25.44; SD = 4.03; Range = 17-33

Table 1: Participant demographic and behavioural data. SD = Standard Deviation. * = behavioural scores significantly greater in ASD>control group, t-test, p<.05.

Behavioural Assessments

General non-verbal intelligence was assessed using the Raven's Matrices Task [28]. The severity of autistic traits was assessed using the Autism Quotient (AQ) and sensory traits using the Glasgow Sensory Questionnaire (GSQ) [29]. Both AQ and GSQ scores were significantly higher in the ASD group (see Table 1). Participants also completed the Mind in the Eyes test [30], however there were no between group differences for this test. The Mind in the Eyes test has been recently criticised for measuring emotion recognition rather than an autism-specific deficit in mental state attribution [31], and therefore these scores were not used to investigate correlations between brain patterns and questionnaire measures.

Paradigm

Whilst undergoing MEG, participants performed an engaging sensory task. Each trial started with a randomised fixation period (1.5, 2.5 or 3.5s), followed by the presentation of a visual grating or auditory binaural click train stimulus. Only the auditory clicktrain data will be described in this article (please see Seymour et al., 2019 [13] for analysis of the visual grating data). The auditory clicktrain was created from auditory square wave clicks, each of 2ms duration delivered every 25ms for a total of 1.5s. Clicktrains were presented at 80dB binaurally through Etymotic MEG-compatible ear tubes. To keep participants engaged with the task, cartoon pictures of aliens or astronauts were presented after the auditory clicktrain, for a maximum of 0.5s. Participants were instructed to press a response-pad as soon as they were presented with a picture of an alien, but not if they were presented with a picture

of an astronaut (maximum response duration allowed was 1.0s). Correct versus incorrect responses were conveyed through 0.5s-long audio-visual feedback (correct: green box, high auditory tone; incorrect responses: red box, low auditory tone). Prior to MEG acquisition, the nature of the task was fully explained to participants and several practice trials were performed. MEG recordings lasted 12-13 minutes and included 64 trials with auditory clicktrain stimuli. Accuracy of picture classification was above 95% for all participants.

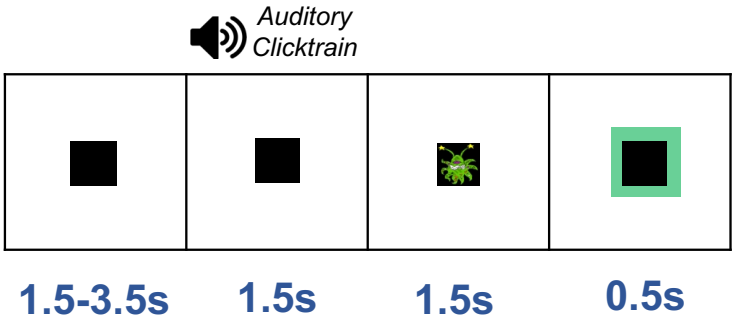

Figure 1. (A) Participants performed an audiovisual task, consisting of 1.5–3.5 s baseline period followed by presentation of an auditory clicktrain stimulus for a duration of 1.5s. After this, participants were presented with a cartoon alien or astronaut picture and instructed to only respond when an alien was presented (response time up to 1.5 s), followed by a green or a red framed box for a correct or an incorrect response, respectively. The alien/astronaut stimuli were to maintain attention and do not form part of the analysed data.

MEG Acquisition

MEG data were acquired using a 306-channel Neuromag MEG scanner (Vectorview, Elekta, Finland) made up of 102 triplets of two orthogonal planar gradiometers and one magnetometer. All recordings were performed inside a magnetically shielded room at a sampling rate of 1000Hz. Five head position indicator (HPI) coils were applied for continuous head position tracking, and visualised post-acquisition using an in-house Matlab script. For MEG-MRI coregistration purposes, the locations of three anatomical landmarks, the locations of the HPI coils and 300-500 points from the head surface were acquired using a Polhemus Fastrak digitizer.

Structural MRI

A structural T1 brain scan was acquired for source reconstruction using a Siemens MAGNETOM Trio 3T scanner with a 32-channel head coil (TE=2.18ms, TR=2300ms,

TI=1100ms, flip angle=9°, 192 or 208 slices depending on head size, voxel-size = 0.8x0.8x0.8cm).

MEG-MRI Coregistration and Cortical Mesh Construction

MEG data were co-registered with participants' structural MRIs by matching the digitised head-shape data with surface data from the structural scan [32]. Two control participants did not complete a T1 structural MRI and therefore a size-matched, template-MRI was used [33,34]. The aligned MRI-MEG images were used to create a forward model based on a single-shell description of the inner surface of the skull [35], using the segmentation function in SPM8 [36]. The cortical mantle was then extracted to create a cortical mesh, using Freesurfer v5.3 [37], and registered to a standard *fs_LR* mesh, based on the Conte69 brain [38], using an interpolation algorithm from the Human Connectome Project [39] (also see: https://goo.gl/3HYA3L). Finally, the mesh was downsampled to 4002 vertices per hemisphere.

MEG Pre-Processing

MEG data were pre-processed using Maxfilter (temporal signal space separation, .9 correlation), which supresses external sources of noise from outside the head [40]. Further pre-processing steps were performed in Matlab 2014b using the Fieldtrip toolbox v20161024 [41]. Firstly, for each participant the entire recording was band-pass filtered between 0.5-250Hz (Butterworth filter, low-pass order 4, high-pass order 3) and band-stop filtered (49.5-50.5Hz; 99.5-100.5Hz) to remove residual 50Hz power-line contamination and its harmonic. Data were epoched into segments of 4000ms (1.5s pre, 1.5s post stimulus onset, with 0.5s of padding either side) and each trial was demeaned and detrended. Trials containing artefacts (SQUID jumps, eye-blinks, head movement, muscle) were removed if the trial-by-channel (magnetomer) variance exceeded $8x10^{-23}$, resulting in the rejection, on average, of 3.4 trials per participant. Four MEG channels containing large amounts of non-physiological noise were removed from all analyses.

Source-Level Spectral Power

Source analysis was conducted using a linearly constrained minimum variance beamformer [42], which applies a spatial filter to the MEG data at each vertex of the cortical mesh. Both sensor types (magnetometers and gradiometers) were used for beamforming. Due to differences in noise between sensor-types, covariance matrix terms resulting from multiplying magnetomer and gradiometer data were removed. Beamformer weights were calculated by combining this covariance matrix with leadfield information, with data pooled across baseline and clicktrain periods (see Figure 1A). Based on recommendations for

optimisation of MEG beamforming [43], a regularisation parameter of lambda 5% was applied.

Whilst the tGBR and ASSR originate from primary auditory cortex, both responses have different frequency ranges and underlying neural generators [25]. Therefore we opted to use separate spatial filters, rather than single spatial filter based on the M100 as used in previous studies [2,44,45]. This was based on recent work suggesting that beamformer weights should be optimised for specific data of interest [46].

To localise the ASSR, data were band-pass filtered (Butterworth filter) between 35-45Hz. To capture induced rather than evoked visual activity, a period of 0.3-1.5s following stimulus onset was compared with a 1.2s baseline period (1.5-0.3s before clicktrain onset). This avoids high-amplitude early-onset event-related fields such as the N100, occurring at 100ms post-clicktrain onset, which could bias source localisation (see below). To localise the tGBR, data were band-pass filtered between 30-60Hz, and a period of 0.05-0.3s following clicktrain onset was compared with a 0.25s baseline period (also see Supporting Figure 2).

Beamformers have been shown to be affected by correlated neural sources (e.g. bilateral auditory responses). Therefore, we opted to compute the covariance matrix on individual trials, rather than trial-averaged data (sensor-level data will be made more ‘correlated’ by averaging over trials). This procedure has been shown to produce sensible bilateral auditory localisations (see: https://bit.ly/2GrB1mj). Results of the source analysis closely resembled the sensor-level data (see Supporting Figure 2), and it is therefore unlikely that group differences were driven by differences in correlated sources.

ROI definition

After confirming that the ASSR localised to temporo-parietal brain regions overlapping with Heschl's gyrus and superior temporal gyrus (see Figure 2), regions of interest (ROI) were selected in bilateral primary auditory (A1) cortices to investigate time-frequency responses in greater detail. ROIs were defined using a multi-modal parcellation from the Human Connectome Project (Supporting Figure 1, [47]). To obtain a single spatial filter for each ROI (right A1 and left A1 separately), we performed a principal components analysis on the concatenated filters of each ROI, multiplied by the sensor-level covariance matrix, and extracted the first component, see [48]. Broadband (0.5-250Hz) sensor-level data were multiplied by this spatial filter to obtain “virtual electrodes”.

A1 Spectral Power

A1 gamma power (ASSR, tGBR) was analysed using the multi-taper method, as implemented in the Fieldtrip toolbox [41]. This has been shown to offer an optimal trade-off between time and frequency resolution, and is preferred to Morlet wavelets for high-frequency gamma-band activity [49,50]. Oscillatory power was calculated from 30-60Hz using a 0.5s sliding window (step size 0.02s) with ±8Hz frequency smoothing.

Statistical comparisons: active>baseline; and control>ASD, were performed using cluster-based permutation tests [51].

A1 Inter-trial Coherence

Inter-trial coherence (ITC) is a measure of band-limited phase consistency across trials. An ITC value of 0, indicates complete absence of phase consistency, whereas a value of 1 indicates perfect phase consistency across trials. At each time *t* and frequency *f*, and for each trial *k*, ITC is calculated [21] as:

$$ITC_{t,f} = \frac{1}{k}\sum_{n=1}^{k} e^{-i\varphi k(t,f)},$$

Statistical comparisons: active>baseline; and control>ASD (baseline-corrected), were performed using cluster-based permutation tests [51].

Statistical Analysis

For MEG data, statistical analysis was performed using cluster-based permutation tests as implemented in the Fieldtrip toolbox, which have been shown to adequately control the type-I error rate for electrophysiological data [51]. Cluster permutation tests consist of two parts: first an uncorrected independent t-test is performed, and all values exceeding a 5% significance threshold are grouped into clusters. The maximum t-value within each cluster is carried forward. Second, a null distribution is obtained by randomising the condition label (e.g. ASD/TDC) 1000 times and calculating the largest cluster-level t-value for each permutation. The maximum t-value within each original cluster is then compared against this null distribution, with values exceeding a threshold (we use $p<.05$) deemed significant.

Results

ASSR – Power

Whilst ASSRs are known to originate from bilateral primary auditory cortex [19,52], in order to confirm successful source localisation with our pipeline, ASSR power (35-45Hz) was localised on a cortical mesh, using an LCMV beamformer, see Methods. We then calculated the percentage change in 35-45Hz power between 0.3-1.5s post-clicktrain onset and a 1.2s baseline period. As expected, the control group showed maximal increases in power for regions overlapping bilateral primary auditory cortex (Figure 2A bottom panel) [20,23]. For the ASD group, there were increases in ASSR power for right, but not left, auditory regions, albeit with lower average values than controls (Figure 2B bottom panel). For an alternative visualisation of results featuring un-thresholded whole-brain statistical maps, see Supporting Information, Figure 4.

Having determined the cortical generators of the ASSR, ROIs were defined in bilateral auditory cortex (see Supporting Figure 1), to investigate time-frequency responses in greater detail. Oscillatory power was calculated in steps of 0.02s using the multitaper method, and post-stimulus periods (0-1.5s) were statistically compared to baseline periods (-1.5 to 0s). Control participants showed bilateral increases in power from 0.1-1.5s, 35-45Hz (Figure 2A top panel), whereas the ASD group only showed increased power in right A1 (Figure 2B top panel). Statistically comparing groups, it was found that the control group had higher 35-45Hz power in both right A1 (Figure 3A, $p<.05$) and left A1 (Figure 3A, $p<.05$) than the ASD group.

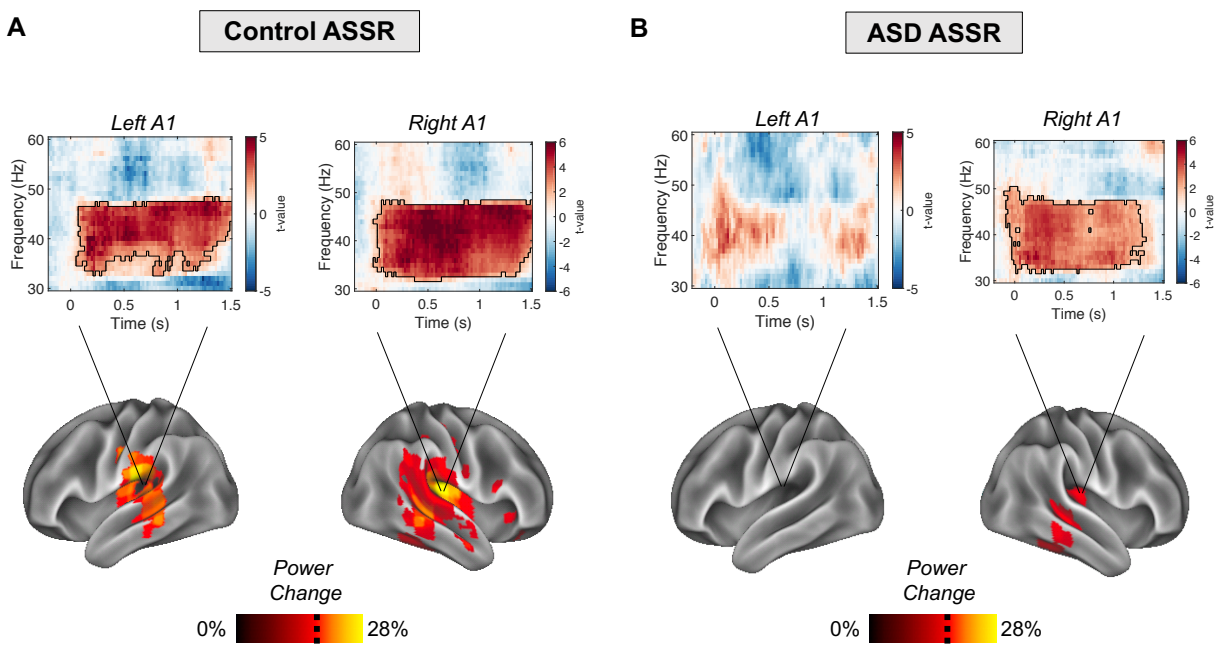

Figure 2. ***Bottom panels (A, B):*** *ASSR beamformer localisations. The percentage change in ASSR power (35-45Hz) is presented on a 3D cortical mesh, thresholded at t > 19% (black dotted line) for illustrative purposes, separately for control* ***(A)*** *and ASD* ***(B)*** *groups.* ***Top-panels (A, B): ASSR in*** *Regions of Interest (ROIs). ROIs were defined in left and right A1 (see Supporting Figure 1) and ASSR oscillatory power was analysed using a time-frequency approach in left and right primary auditory cortex, A1 (see Methods for details).* ***(A)*** *The control group showed significantly increased ASSR power (p<.05) compared to pre-stimulus baseline between 35-45Hz in left and right A1.* ***(B)*** *In contrast, the ASD group only showed significantly increased ASSR power compared to baseline for right A1. ASSR = Auditory Steady State Response.*

Next, we ran an exploratory post-hoc analysis to investigate hemispheric differences in the ASSR. For each ROI and participant, we calculated the percentage change in ASSR power from 35-45Hz, between 0.4-1.5s post-clicktrain onset and a 1.1s baseline period. These values were entered into a 2x2 ANOVA, with group (ASD, control) and hemisphere (left, right) as factors. Results showed a significant main effect of group, $F(1, 68) = 21.22$, $p<.001$, $\eta^2 = .12$, and hemisphere $F(1,68) = 15.63$, $p<.001$, $\eta^2 =0.15$, but not a group*hemisphere interaction, $F(1,68) = 1.780$, $p=.19$, $\eta^2 = .017$. This suggests that the reduced ASSR power for the ASD group was not a function of hemisphere (Figure 3B).

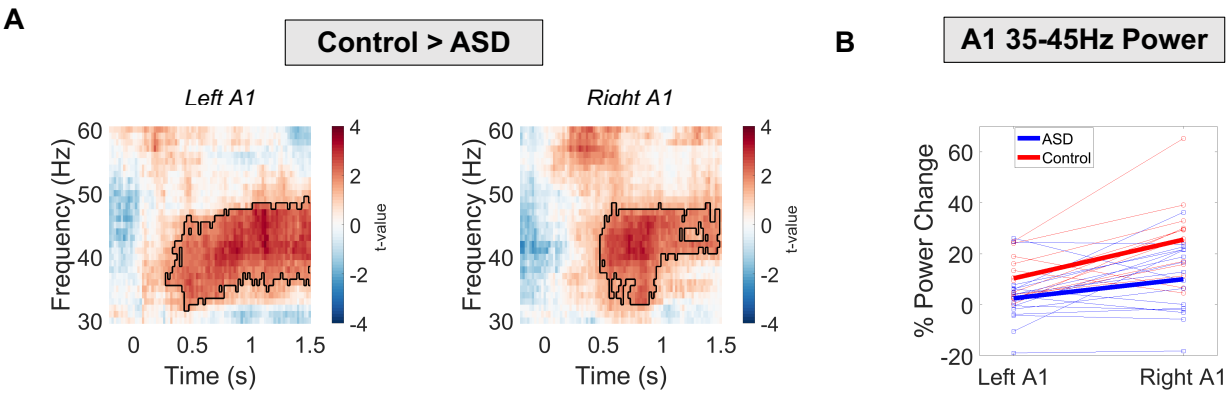

Figure 3. ***(A)*** *By statistically comparing groups over time and frequency, it was found that the control group had greater ASSR power than the ASD group from 0.5-1.5s in left A1 (p=.024) and from 0.4-1.5s in right A1(p=.011), , ,.* ***(B)*** *For left and right A1, the percentage change in ASSR power was calculated for 0.4-1.5s post-clicktrain onset versus a 1.1s baseline period. Data from each hemisphere and group is plotted separately (ASD: blue line; controls: red line). Thick lines represent the group mean whereas thinner lines represent individual data-points.*

ASSR – Intertrial Coherence (ITC)

Next, inter-trial coherence (ITC) was calculated for the A1 ROIs, using the same time-frequency approach as for power. We statistically compared post-clicktrain time-periods (0-1.5s) to baseline time-periods (-1.5-0s) which results in ITC values being converted to t-values. Both groups of participants showed statistically significant, p<.05, increases in ITC from 0.1-1.5s, 38-42Hz, across both left and right A1 (Figure 4A-B). Statistical comparison of ITC between groups showed that the control group had higher ITC in both right A1 (Figure 4C, p=.038) and left A1 (Figure 4D, p=.020), but only within a time-window ranging from 0.5-1.0s post-stimulus onset.

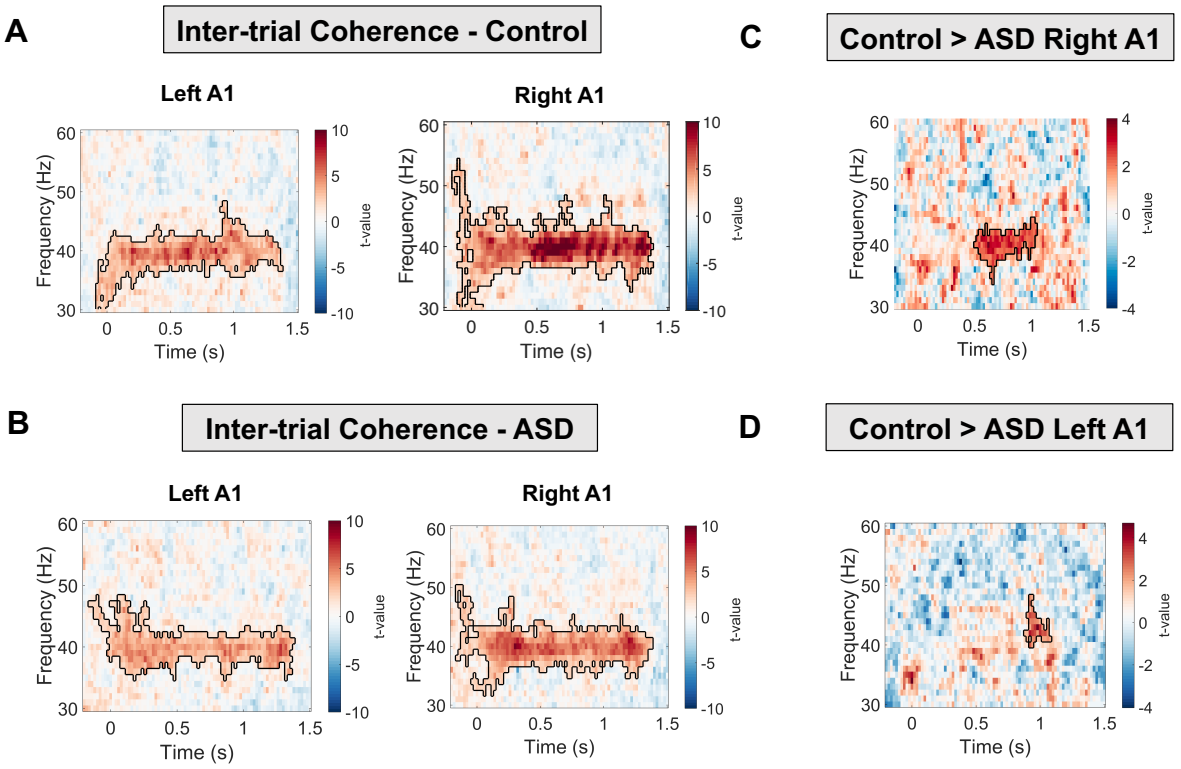

Figure 4. ASSR inter-trial coherence (ITC) was analysed across time (0-1.5s) and frequency (30-60Hz) in left and right primary auditory cortex, A1. ***(A-B)*** *Both groups showed increased ASSR ITC between 37-48Hz in left and right A1.* ***(C-D)*** *Statistical comparison across groups revealed that the control group had significantly (p<.05) higher ASSR ITC from 0.4-1.0s for right A1, and 0.9-1.11s for left A1.*

ASSR – Behavioural Data

Next we investigated whether ASSR responses in the ASD group were correlated with behavioural questionnaire data collected from participants. To do this, the percentage change in ASSR power (0.4-1.5s, averaged over left and right A1) and ITC values (0.5-1.0s, averaged over left and right A1), were correlated with Autism Quotient (AQ) and Glasgow Sensory Questionnaire (GSQ) data, for the ASD group. However, there were no significant correlations for either AQ (Figure 5A, r = .14, p = .586; Figure 5C, r = -.134, p =.596) or GSQ (Figure 5B, r = -.22, p = .381, r = -.180 , p = .475; Figure 5D).

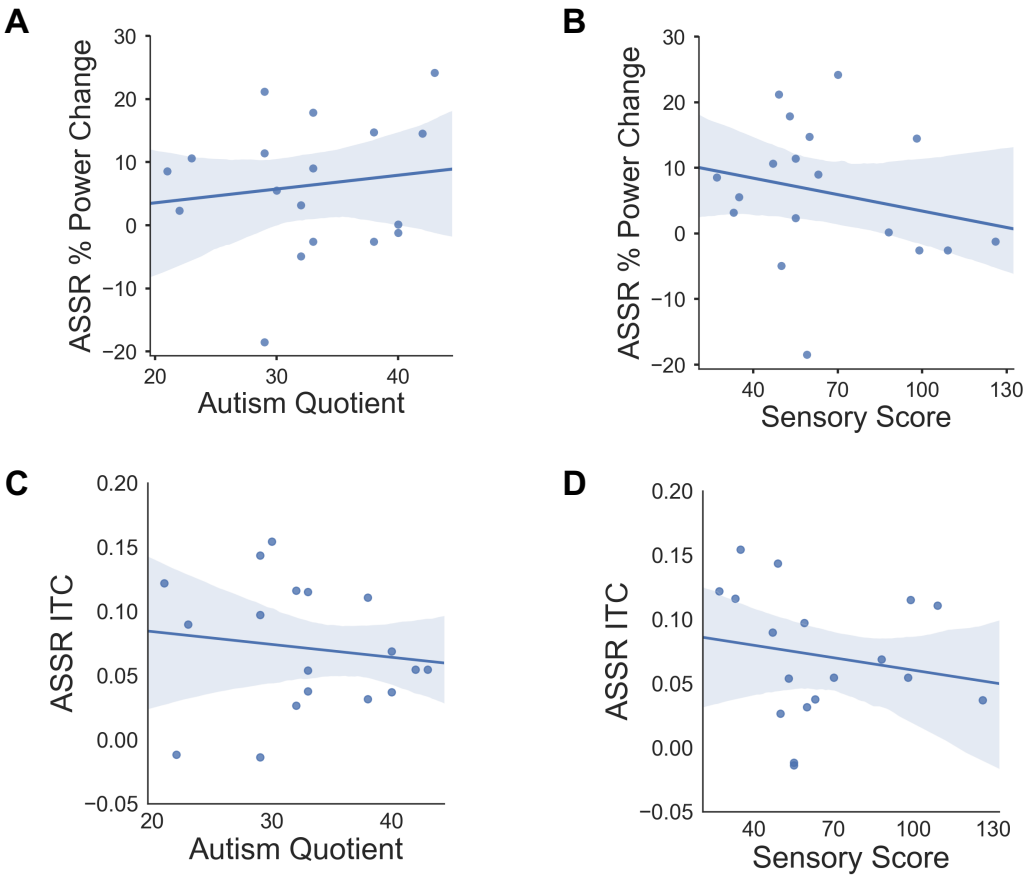

Figure 5. ***(A-B)*** *Scatter plots to show the relationship between ASSR power, averaged across left and right A1, and Autism Quotient and Sensory Scores.* ***(C-D)*** *Scatter plots to show the relationship between ASSR ITC, averaged across left and right A1, and Autism Quotient and Sensory Scores. There were no significant (p>.05) correlations for any brain-behaviour relationship. The shaded region indicates 95% confidence intervals. ITC = Intertrial Coherence; ASSR = Auditory Steady State Response.*

tGBR – Source-Level

Transient gamma-band responses to the auditory clicktrain were localised using a beamforming approach (see Methods). As for the ASSR analysis, we first confirmed that the cortical generator(s) of the ASSR originated in bilateral auditory cortex. We calculated the percentage change in 30-60Hz power from 0.05-0.3s post-clicktrain onset compared with a 0.25 baseline period [51]. As expected, both groups group showed maximal increases in tGBR power for regions overlapping with bilateral primary auditory cortex (Figure 2A-B) [20,23]; although tGBR power for the control group was less pronounced in the right hemisphere.

Paralleling the ASSR analysis, ROIs were defined in left and right A1. For each ROI and participant, we calculated the percentage change in tGBR power from 30-60Hz, between 0.05-0.3s post-clicktrain onset and for a 0.25s baseline period. These values were entered into a 2x2 ANOVA, with group and hemisphere as factors (Figure 6C). Results showed no significant main effect of: group, $F(1, 68) = 0.681$, $p=.41$, $\eta^2 = .010$; hemisphere, $F(1,68) = 0.252$, $p=.62$, $\eta^2 = .004$; and no significant group*hemisphere interaction, $F(1,68) = 0.651$, $p=.42$, $\eta^2 = .009$. This suggests that tGBRs are not significantly different across groups or hemispheres.

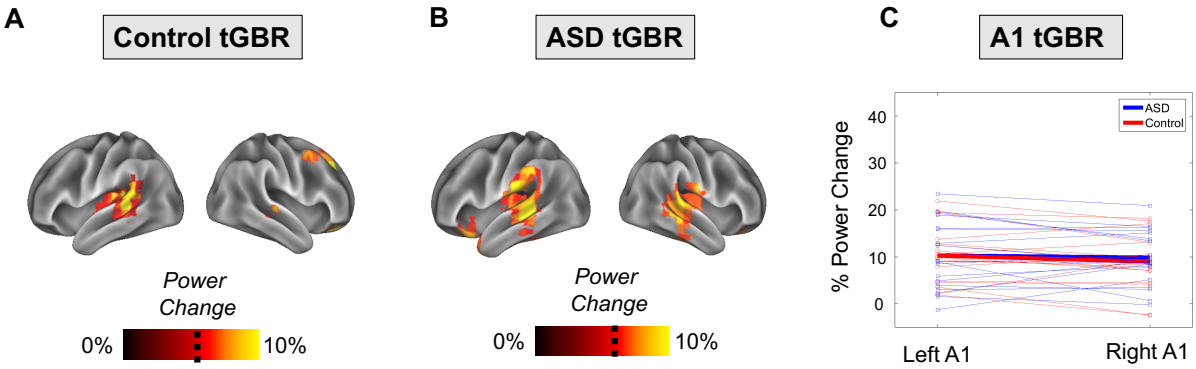

*Figure 6. The percentage change in transient gamma-band resonse, tGBR, power (30-60Hz) is presented on a 3D cortical mesh, thresholded at t > 5.6% (dotted black line) for illustrative purposes, separately for control **(A)** and ASD **(B)** groups. **(C)** tGBR was plotted separately across hemispheres and group (ASD: blue line; controls: red line). Thick lines represent the group mean whereas thinner lines represent individual data-points.*

Discussion

This study examined the oscillatory basis of auditory steady state responses (ASSRs) and transient gamma-band responses (tGBR) in a group of 18 autistic adolescents and 18 typically developing controls. We utilised robust source-localisation methods and analysed auditory responses across both frequency *and* time. Compared to the ASSR in the control group, we found reduced ~40Hz power for the ASD group, for regions of interest defined in the left and right primary auditory cortices. Furthermore, there was reduced inter-trial coherence for the autistic group at 40Hz, suggesting that phase dynamics in A1 were less consistent over time. Our results corroborate the notion that auditory brain responses in autism are locally dysregulated [7], especially during sustained gamma-band entrainment (<0.4s).

Auditory Steady State Responses (ASSR) in Autism

Our results are largely consistent with two previous studies which show reduced ASSRs in autistic adolescents [2] and first-degree relatives of people diagnosed with autism [1]. Whilst our study shows reductions in 40Hz power across *both* hemispheres (Figure 2-3), Wilson & colleagues (2007), observed a selective *left*-hemisphere reduction in power [2]. This might be due to the monaural stimulation approach, used by Wilson & colleagues (2007), producing larger hemispheric asymmetries as compared to binaural auditory stimulation [53]. Future work is clearly needed to clarify hemispheric asymmetries in ASSR power for ASD populations [53].

Our results build on the previous literature in several ways. Firstly, by examining sustained ASSRs from 0-1.5s we found that group differences emerged beyond 0.4s post-stimulus onset (Figure 2-3), suggesting that, when driven at gamma frequencies, A1 becomes increasingly dysregulated in ASD compared to controls in a time-dependent manner. This raises the intriguing possibility that sustained, rather than transient, oscillatory activity at gamma-frequencies is affected in autism, perhaps reflecting synaptic dysfunction and an imbalance between excitatory and inhibitory populations of neurons [16]. To investigate this further, future work could parametrically modulate clicktrain duration, intensity, and variability (e.g. perfect 40 Hz vs 38-42Hz, etc.). Secondly, our results were complimented by measures of ITC, which showed reduced phase consistency in the autistic group from 0.5-1.0s post-stimulus onset (Figure 5) that was most pronounced in right A1. Reduced phase consistency may reflect more idiosyncratic neural responses in autism [54,55], as previously reported for evoked data [56]. Importantly, measures of ITC are normalised by amplitude and more robust to data with lower signal-to-noise ratios [23]. Therefore, the correspondence between power and ITC, albeit in a smaller time-window for ITC, strengthens the claim of reduced ASSRs in autism.

Transient Gamma-Band Responses in Autism

Unlike ASSRs, there were no group differences in the transient gamma-band (30-60Hz) responses to the clicktrain stimulus (Figure 6). Whilst one previous study using sinusoidal tones reported decreased tGBRs for the first-degree relatives of autistic people, a later study using auditory clicktrains, found no group differences in either power or ITC [1]. More generally, findings of transient/evoked gamma-band power across sensory domains are very mixed, with both increases and decreases reported (reviewed in [7]). The divergence between steady-state and transient gamma in this study has implications for potential oscillopathies in ASD, as differences in gamma power may depend on the time-period under investigation as well as the underlying neural circuits generating gamma oscillations [25].

ASSRs as Markers of Dysregulated Local Activity

There has been recent interest in characterising atypical patterns of gamma-band oscillations in autism, due to their link with local cortical function and connectivity [7]. The precise E-I mechanisms underlying gamma generation are well characterised, for a review see [14]. Of particular importance is the functional inhibition of pyramidal neurons by fast-spiking interneurons via binding of the neurotransmitter gamma-aminobutyric acid (GABA) [14,57]. Relatedly, there is emerging evidence showing GABA dysfunction in autism [57]. Reduced gamma-band steady-state responses in autism may therefore reflect dysregulated neuronal inhibition, resulting in E-I imbalance [16]. To quantify the precise mechanisms underlying reduced gamma-band ASSRs, future studies could utilise dynamic causal modelling of A1 neuronal circuits [58], combined with parametric modulations of ASSRs (e.g. duration, frequency) and participant attention [59].

It should also be noted that ASSRs are not simply generated via the linear accumulation of transient evoked responses [20,60,61]. Instead, the ASSR may reflect a sustained non-linear neural response at the input stimulation frequency and its harmonics, peaking at the system's preferred modulation rate [20]. In support of this, Edgar & colleagues (2016) report that in children, ASSRs are difficult to detect, despite measurable auditory evoked responses [25]. Similarly, our data show intact auditory evoked fields (see Supporting Figure 2) and transient gamma-band responses in autism (Fig. 6), in the presence of a reduced ASSR (Fig. 3). Rather than a generalised gamma-band dysfunction in autism, our data suggest a more nuanced reduction in the non-linear dynamics underlying steady-state auditory gamma [1]. Interestingly, an MEG study examining somatosensory processing in ASD showed reduced frequency harmonics at 50Hz [12], while Vilidaite and colleagues reported a reduction in harmonic EEG responses during visual steady-state stimulation in autistic adults [62]. Furthermore, two MEG studies revealed reduced alpha-gamma phase-amplitude coupling in the visual system in ASD [14, 18]. Overall, this suggests that non-linear aspects of local cortical processing could be dysregulated across sensory domains in ASD [8].

ASSRs are developmentally relevant, increasing by approximately 0.01 ITC value per year [24,25,44]. This trajectory may reflect the continuing development of superficial layers of cortex where gamma-band oscillations predominantly originate [27]. We hypothesise that the ASD-related reduction in ASSRs reported in this study results from an atypical trajectory of gamma-band maturation, in line with developmental disconnection theories of autism [63]. To investigate this further, future studies could use high powered longitudinal ASD samples, to characterise ASSR development throughout childhood and adolescence [64]. If

confirmed, divergent ASSR trajectories could act as important autism-relevant markers of intervention efficacy [65].

Limitations

We did not collect a formal clinical assessment of autism from our participants, e.g. the ADOS [66]. We therefore implemented strict participant exclusion criteria, only including autistic participants with a confirmed clinical diagnosis of ASD or Asperger's syndrome. Between groups, there were significant differences in autistic and sensory traits, measured using two self-report questionnaires (Table 1). However, upon closer inspection of behavioural data (see Supporting Figure 4), the ASD group showed a mixture of hyper- and hypo-sensitive traits between different sensory modalities making precise brain-behavioural correlations problematic. This may explain the lack of relationship between ASSR power/ITC and AQ/GSQ scores in ASD (Figure 5). Brain-behaviour relationships might be better quantified using MEG in combination with psychophysical tests of auditory perception and formal clinical assessments.

Declarations

Ethics approval and consent to participate

All experimental procedures complied with the Declaration of Helsinki and were approved by the Aston University, Department of Life & Health Sciences ethics committee. Participants and a parent/guardian gave written informed consent before participating in the study.

Consent for publication

N/A

Availability of data and materials

The data that support the findings of this study are available on reasonable request from corresponding author, R.S., in a preprocessed and de-anonymized form. The raw data are not publicly available due to ethical restrictions.

Competing Interests

The authors wish to declare the research was conducted in the absence of any commercial or financial relationships that could be construed as a potential conflict of interest.

Funding

The Wellcome Trust, Dr Hadwen Trust and Tommy's Fund supported research-scanning costs. Robert Seymour was supported by a cotutelle PhD studentship from Aston University and Macquarie University**.**

Author Contributions

RS: Study design; data collection; data analysis; data interpretation; manuscript writing.

KK: Study design; data interpretation; manuscript writing.

GR: Study design; data interpretation; manuscript writing.

PFS: Data interpretation; manuscript writing.

GGW: Data collection; data interpretation.

Acknowledgments

We wish to thank: the volunteers who gave their time to participate in this study; Dr Shu Yau and Dr. Michael Hall for help with MRI data acquisition; and Dr Jon Brock for intellectual contributions to experimental design.

References

1. Rojas DC, Teale PD, Maharajh K, Kronberg E, Youngpeter K, Wilson LB, et al. Transient and steady-state auditory gamma-band responses in first-degree relatives of people with autism spectrum disorder. Mol Autism. 2011;2:11.

2. Wilson TW, Rojas DC, Reite ML, Teale PD, Rogers SJ. Children and adolescents with autism exhibit reduced MEG steady-state gamma responses. Biol Psychiatry. 2007;62:192–197.

3. American Psychological Association. Diagnostic and statistical manual of mental disorders . Arlington: American Psychiatric Association; 2013.

4. Hazen EP, Stornelli JL, O'Rourke JA, Koesterer K, McDougle CJ. Sensory symptoms in autism spectrum disorders. Harv Rev Psychiatry. 2014;22:112–124.

5. Leekam SR, Nieto C, Libby SJ, Wing L, Gould J. Describing the sensory abnormalities of children and adults with autism. J Autism Dev Disord. 2007;37:894–910.

6. Robertson CE, Baron-Cohen S. Sensory perception in autism. Nat Rev Neurosci. 2017;18:671.

7. Kessler K, Seymour RA, Rippon G. Brain oscillations and connectivity in autism spectrum disorders (ASD): new approaches to methodology, measurement and modelling. Neurosci Biobehav Rev. 2016;71:601–20.

8. Roberts TP, Khan SY, Rey M, Monroe JF, Cannon K, Blaskey L, et al. MEG detection of delayed auditory evoked responses in autism spectrum disorders: towards an imaging biomarker for autism. Autism Res. 2010;3:8–18.

9. Simon DM, Wallace MT. Dysfunction of sensory oscillations in Autism Spectrum Disorder. Neurosci Biobehav Rev. 2016;68:848–61.

10. Brown C, Gruber T, Boucher J, Rippon G, Brock J. Gamma abnormalities during perception of illusory figures in autism. Cortex. 2005;41:364–376.

11. Wright B, Alderson-Day B, Prendergast G, Bennett S, Jordan J, Whitton C, et al. Gamma activation in young people with autism spectrum disorders and typically-developing controls when viewing emotions on faces. PLoS One. 2012;7:e41326.

12. Khan, Michmizos K, Tommerdahl M, Ganesan S, Kitzbichler MG, Zetino M, et al. Somatosensory cortex functional connectivity abnormalities in autism show opposite trends, depending on direction and spatial scale. Brain. 2015;138:1394–409.

13. Seymour RA, Rippon G, Gooding-Williams G, Schoffelen JM, Kessler K. Dysregulated oscillatory connectivity in the visual system in autism spectrum disorder. Brain. 2019; 142:3294–3305.

14. Buzsáki G, Wang X-J. Mechanisms of gamma oscillations. Annu Rev Neurosci. 2012;35:203.

15. Fries P. Rhythms for cognition: communication through coherence. Neuron. 2015;88:220–235.

16. Rubenstein JLR, Merzenich MM. Model of autism: increased ratio of excitation/inhibition in key neural systems. Genes Brain Behav. 2003;2:255–267.

17. Khan S, Gramfort A, Shetty NR, Kitzbichler MG, Ganesan S, Moran JM, et al. Local and long-range functional connectivity is reduced in concert in autism spectrum disorders. Proc Natl Acad Sci. 2013;110:3107–12.

18. Pantev C. Evoked and induced gamma-band activity of the human cortex. Brain Topogr. 1995;7:321–330.

19. Hari R, Hämäläinen M, Joutsiniemi S-L. Neuromagnetic steady-state responses to auditory stimuli. J Acoust Soc Am. 1989;86:1033–1039.

20. Pantev C, Roberts LE, Elbert T, Roβ B, Wienbruch C. Tonotopic organization of the sources of human auditory steady-state responses. Hear Res. 1996;101:62–74.

21. Busch NA, Dubois J, VanRullen R. The phase of ongoing EEG oscillations predicts visual perception. J Neurosci. 2009;29:7869–7876.

22. McFadden KL, Steinmetz SE, Carroll AM, Simon ST, Wallace A, Rojas DC. Test-Retest Reliability of the 40 Hz EEG Auditory Steady-State Response. PLOS ONE. 2014;9:e85748.

23. Tan H-R, Gross J, Uhlhaas PJ. MEG—measured auditory steady-state oscillations show high test–retest reliability: A sensor and source-space analysis. Neuroimage. 2015;122:417–426.

24. Cho RY, Walker CP, Polizzotto NR, Wozny TA, Fissell C, Chen C-MA, et al. Development of sensory gamma oscillations and cross-frequency coupling from childhood to early adulthood. Cereb Cortex. 2015;25:1509–1518.

25. Edgar JC, Fisk CL, Liu S, Pandey J, Herrington JD, Schultz RT, et al. Translating Adult Electrophysiology Findings to Younger Patient Populations: Difficulty Measuring 40-Hz Auditory Steady-State Responses in Typically Developing Children and Children with Autism Spectrum Disorder. Dev Neurosci. 2016; 38:1-14.

26. Moore JK, Guan Y-L. Cytoarchitectural and axonal maturation in human auditory cortex. J Assoc Res Otolaryngol. 2001;2:297–311.

27. Moore JK, Linthicum Jr FH. The human auditory system: a timeline of development. Int J Audiol. 2007;46:460–478.

28. Raven JC, Court JH. Raven's progressive matrices and vocabulary scales . Oxford: Oxford Psychologists Press; 1998.

29. Robertson AE, Simmons DR. The relationship between sensory sensitivity and autistic traits in the general population. J Autism Dev Disord. 2013;43:775–784.

30. Baron-Cohen S, Wheelwright S, Hill J, Raste Y, Plumb I. The "Reading the Mind in the Eyes" test revised version: A study with normal adults, and adults with Asperger syndrome or high-functioning autism. J Child Psychol Psychiatry. 2001;42:241–251.

31. Oakley BF, Brewer R, Bird G, Catmur C. Theory of mind is not theory of emotion: A cautionary note on the Reading the Mind in the Eyes Test. J Abnorm Psychol. 2016;125:818.

32. Jenkinson M, Smith S. A global optimisation method for robust affine registration of brain images. Med Image Anal. 2001;5:143–56.

33. Gohel B, Lim S, Kim M-Y, Kwon H, Kim K. Approximate Subject Specific Pseudo MRI from an Available MRI Dataset for MEG Source Imaging. Front Neuroinformatics. 2017;11:50.

34. Seymour R. Macquarie-MEG-Research/MEMES: For Zenodo [Internet]. 2018. Available from: https://doi.org/10.5281/zenodo.1451031

35. Nolte G. The magnetic lead field theorem in the quasi-static approximation and its use for magnetoencephalography forward calculation in realistic volume conductors. Phys Med Biol. 2003;48:3637–52.

36. Litvak V, Mattout J, Kiebel S, Phillips C, Henson R, Kilner J, et al. EEG and MEG data analysis in SPM8. Comput Intell Neurosci. 2011.

37. Fischl B. FreeSurfer. Neuroimage. 2012;62:774–781.

38. Essen V, C D, Glasser MF, Dierker DL, Harwell J, Coalson T. Parcellations and Hemispheric Asymmetries of Human Cerebral Cortex Analyzed on Surface-Based Atlases. Cereb Cortex. 2012;22:2241–62.

39. Van Essen DC, Ugurbil K, Auerbach E, Barch D, Behrens TEJ, Bucholz R, et al. The Human Connectome Project: a data acquisition perspective. Neuroimage. 2012;62:2222–2231.

40. Taulu S, Simola J. Spatiotemporal signal space separation method for rejecting nearby interference in MEG measurements. Phys Med Biol. 2006;51:1759.

41. Oostenveld R, Fries P, Maris E, Schoffelen J-M. FieldTrip: open source software for advanced analysis of MEG, EEG, and invasive electrophysiological data. Comput Intell Neurosci. 2010.

42. Van Veen BD, van Drongelen W, Yuchtman M, Suzuki A. Localization of brain electrical activity via linearly constrained minimum variance spatial filtering. IEEE Trans Biomed Eng. 1997;44:867–80.
43. Brookes MJ, Vrba J, Robinson SE, Stevenson CM, Peters AM, Barnes GR, et al. Optimising experimental design for MEG beamformer imaging. Neuroimage. 2008;39:1788–1802.

44. Rojas DC, Maharajh K, Teale PD, Kleman MR, Benkers TL, Carlson JP, et al. Development of the 40Hz steady state auditory evoked magnetic field from ages 5 to 52. Clin Neurophysiol. 2006;117:110–117.

45. Rojas DC, Teale PD, Maharajh K, Kronberg E, Youngpeter K, Wilson LB, et al. Transient and steady-state auditory gamma-band responses in first-degree relatives of people with autism spectrum disorder. Mol Autism. 2011;2:1.

46. Barratt EL, Francis ST, Morris PG, Brookes MJ. Mapping the topological organisation of beta oscillations in motor cortex using MEG. NeuroImage. 2018;

47. Glasser MF, Coalson TS, Robinson EC, Hacker CD, Harwell J, Yacoub E, et al. A multi-modal parcellation of human cerebral cortex. Nature. 2016;536:171–8.

48. Schoffelen J-M, Hultén A, Lam N, Marquand AF, Uddén J, Hagoort P. Frequency-specific directed interactions in the human brain network for language. Proc Natl Acad Sci. 2017;114:8083–8088.

49. Hoogenboom N, Schoffelen J-M, Oostenveld R, Parkes LM, Fries P. Localizing human visual gamma-band activity in frequency, time and space. Neuroimage. 2006;29:764–773.

50. Muthukumaraswamy SD. High-frequency brain activity and muscle artifacts in MEG/EEG: a review and recommendations. Front Hum Neurosci. 2013.

51. Maris E, Oostenveld R. Nonparametric statistical testing of EEG- and MEG-data. J Neurosci Methods. 2007;164:177–90.

52. Popov T, Oostenveld R, Schoffelen JM. FieldTrip Made Easy: An Analysis Protocol for Group Analysis of the Auditory Steady State Brain Response in Time, Frequency, and Space. Front Neurosci. 2018;12.

53. Ross B, Herdman AT, Pantev C. Right hemispheric laterality of human 40 Hz auditory steady-state responses. Cereb Cortex. 2005;15:2029–2039.

54. Hahamy A, Behrmann M, Malach R. The idiosyncratic brain: distortion of spontaneous connectivity patterns in autism spectrum disorder. Nat Neurosci. 2015;18:302–309.

55. Nunes AS, Peatfield N, Vakorin V, Doesburg SM. Idiosyncratic organization of cortical networks in autism spectrum disorder. Neuroimage. 2018;

56. Dinstein I, Pierce K, Eyler L, Solso S, Malach R, Behrmann M, et al. Disrupted neural synchronization in toddlers with autism. Neuron. 2011;70:1218–1225.
57. Coghlan S, Horder J, Inkster B, Mendez MA, Murphy DG, Nutt DJ. GABA system dysfunction in autism and related disorders: from synapse to symptoms. Neurosci Biobehav Rev. 2012;36:2044–2055.

58. Moran RJ, Stephan KE, Seidenbecher T, Pape H-C, Dolan RJ, Friston KJ. Dynamic causal models of steady-state responses. NeuroImage. 2009;44:796–811.

59. Ross B, Picton TW, Herdman AT, Pantev C. The effect of attention on the auditory steady-state response. Neurol Clin Neurophysiol NCN. 2004;2004:22–22.

60. Azzena GB, Conti G, Santarelli R, Ottaviani F, Paludetti G, Maurizi M. Generation of human auditory steadystate responses (SSRs). I: Stimulus rate effects. Hear Res. 1995;83:1–8.

61. Santarelli R, Maurizi M, Conti G, Ottaviani F, Paludetti G, Pettorossi VE. Generation of human auditory steady-state responses (SSRs). II: Addition of responses to individual stimuli. Hear Res. 1995;83:9–18.

62. Vilidaite G, Norcia AM, West RJ, Elliott CJ, Pei F, Wade AR, et al. Autism sensory dysfunction in an evolutionarily conserved system. Proc R Soc B. 2018;285:20182255.

63. Geschwind DH, Levitt P. Autism spectrum disorders: developmental disconnection syndromes. Curr Opin Neurobiol. 2007;17:103–111.

64. Loth E, Charman T, Mason L, Tillmann J, Jones EJH, Wooldridge C, et al. The EU-AIMS Longitudinal European Autism Project (LEAP): design and methodologies to identify and validate stratification biomarkers for autism spectrum disorders. Mol Autism. 2017;8:24.

65. Mamashli F, Khan S, Bharadwaj H, Losh A, Pawlyszyn SM, Hämäläinen MS, et al. Maturational trajectories of local and long-range functional connectivity in autism during face processing. Hum Brain Mapp. 2018;39:4094–4104.

66. Lord C, Risi S, Lambrecht L, Cook EH, Leventhal BL, DiLavore PC, et al. The Autism Diagnostic Observation Schedule—Generic: A standard measure of social and communication deficits associated with the spectrum of autism. J Autism Dev Disord. 2000;30:205–223.

Supporting Information:

Reduced Auditory Steady State Responses in Autism Spectrum Disorder

Seymour, R.A., Rippon, G., Gooding-Williams, G,. Sowman, P.F. & Kessler, K.

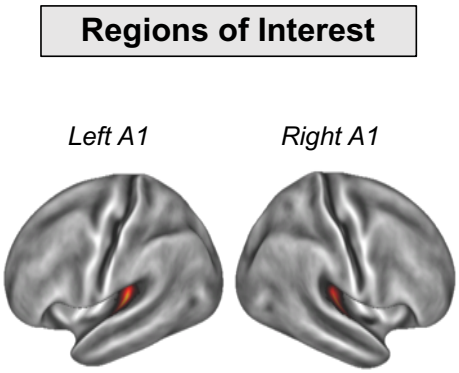

Supporting Figure 1: Regions of interest were defined in left and right Primary Auditory Cortex, according to HCP-MMP 1.0 Atlas.

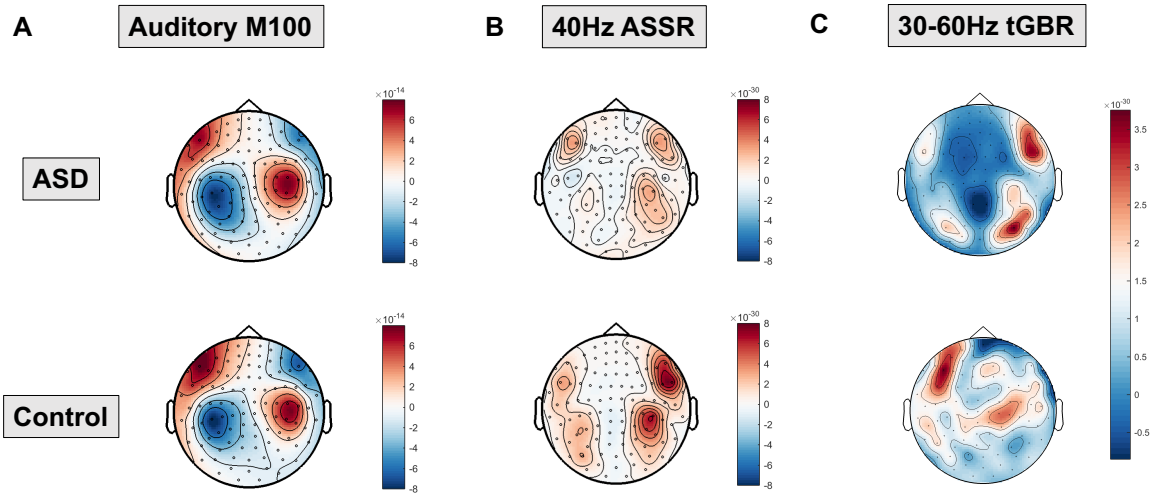

Supporting Figure 2: Sensor-level Analysis. **(A)** Group average topo-plot for the auditory M100 event-related field, magnetometers shown. **(B)** Group average topo-plot for auditory steady state responses (ASSR) at 40Hz **(C)** Group average topo-plot of the transient gamma-band response (tGBR), 30-60Hz, 0.05-0.3s. Scales represent MEG field strength, baseline-corrected, with units of Tesla/cm.

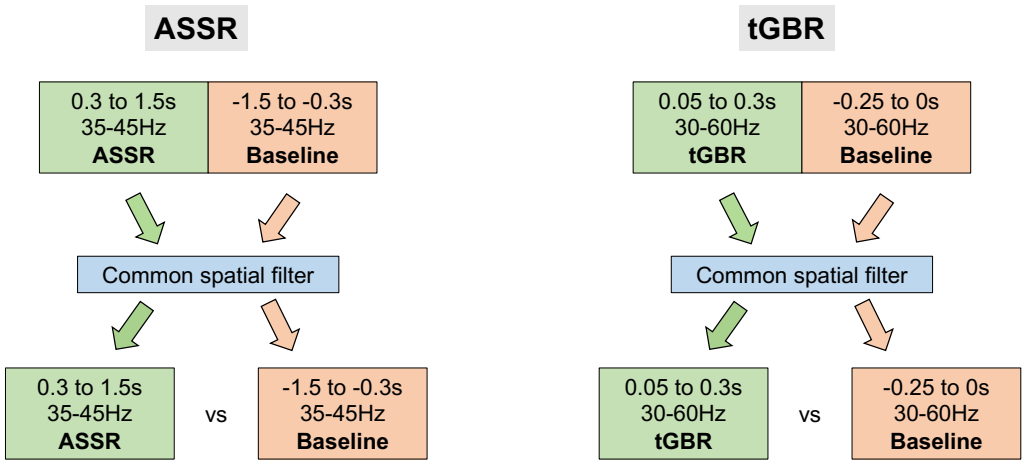

Supporting Figure 3: Procedure for Source Analysis. For ASSR beamforming, a common spatial filter was computed using data pooled across ASSR and baseline data. This common filter was then used to localise ASSR/baseline data separately. This process was repeated for tGBR data, but the common spatial filter was computed using a different time and frequency band of interest.

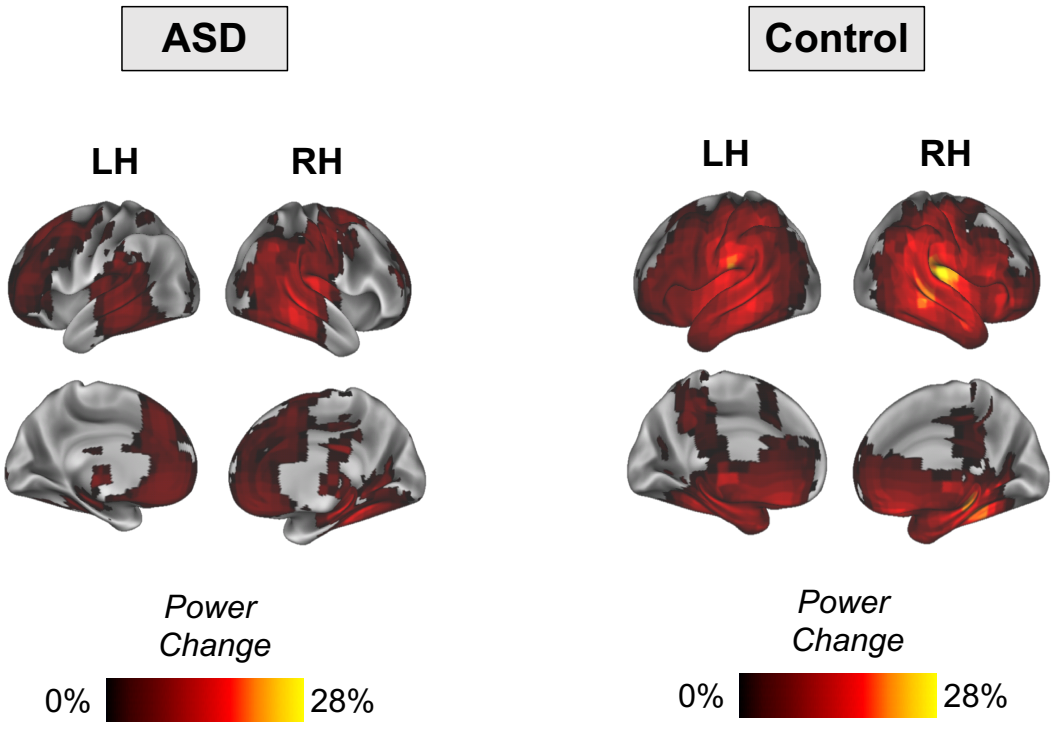

Supporting Figure 4: Whole-brain maps showing changes in ASSR power (positive values only), corresponding to Figure 2.

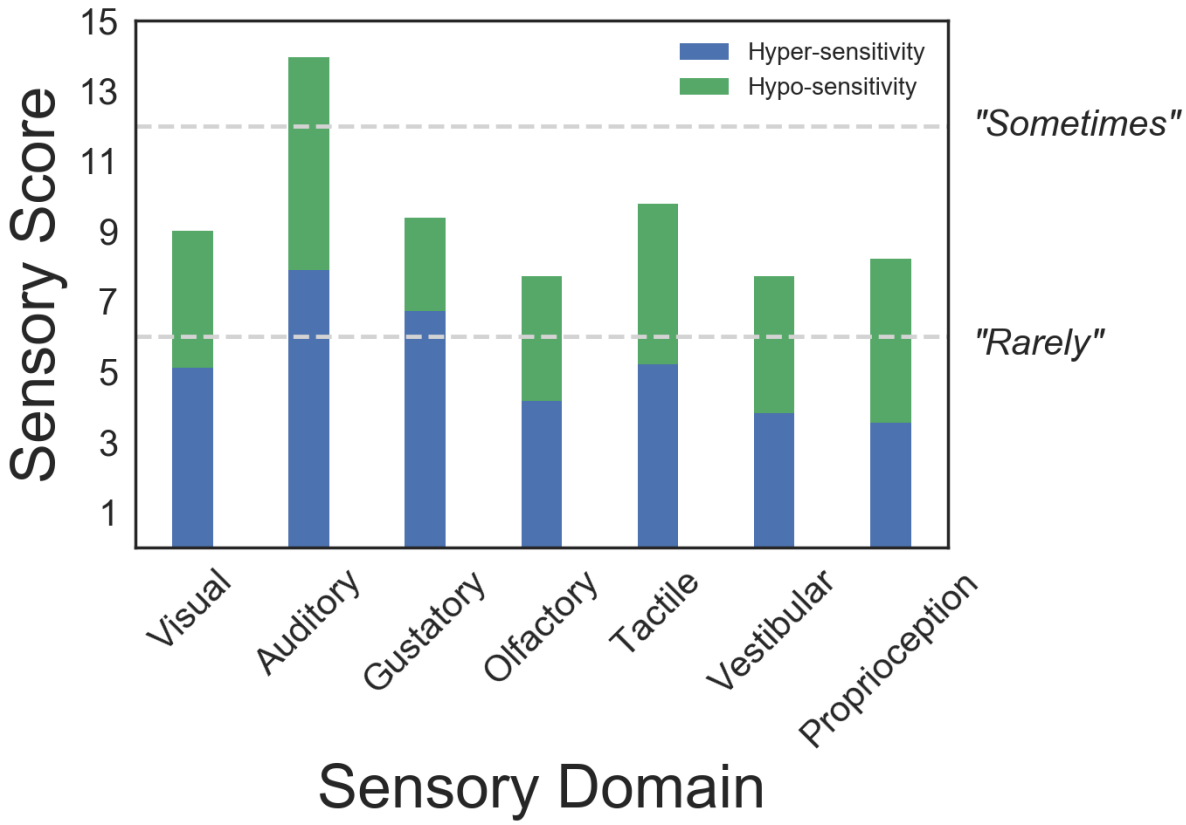

Supporting Figure 5: Responses to the Glasgow Sensory Questionnaire were grouped by sensory domain (maximum score = 20) and hypo- / hyper-sensitivity (green and blue bars respectively). Our data show a heterogeneous pattern of sensory symptoms, with mixture of hypo- and hyper-sensitivities. Visual symptoms scored 9.0/20 corresponding to questionnaire answers between “Rarely” and “Sometimes”. Auditory sensory symptoms were higher than for other modalities.